Theory of Active Intracellular Transport by DNA Relaying

Christian Hanauer,[1,*] Silke Bergeler,[1,*] Erwin Frey,[1] and Chase P. Broedersz[1,2,†]
[1]Arnold-Sommerfeld-Center for Theoretical Physics and Center for NanoScience, Ludwig-Maximilians-Universität München, D-80333 München, Germany
[2]Department of Physics and Astronomy, Vrije Universiteit Amsterdam, 1081 HV Amsterdam, Netherlands

(Received 8 January 2021; accepted 12 August 2021; published 21 September 2021)

The spatiotemporal organization of bacterial cells is crucial for the active segregation of replicating chromosomes. In several species, including *Caulobacter crescentus*, the ATPase ParA binds to DNA and forms a gradient along the long cell axis. The ParB partition complex on the newly replicated chromosome translocates up this ParA gradient, thereby contributing to chromosome segregation. A DNA-relay mechanism—deriving from the elasticity of the fluctuating chromosome—has been proposed as the driving force for this cargo translocation, but a mechanistic theoretical description remains elusive. Here, we propose a minimal model to describe force generation by the DNA-relay mechanism over a broad range of operational conditions. Conceptually, we identify four distinct force-generation regimes characterized by their dependence on chromosome fluctuations. These relay force regimes arise from an interplay of the imposed ParA gradient, chromosome fluctuations, and an emergent friction force due to chromosome-cargo interactions.

DOI: 10.1103/PhysRevLett.127.138101

The interior organization of bacterial cells is an essential prerequisite for several vital processes, ranging from chromosome and plasmid segregation to cell division [1]. Dedicated active mechanisms ensure the rapid translocation and accurate localization of macromolecular objects in the cell [2–5]. A prominent example is the translocation of the partition complex during chromosome segregation in bacteria such as *Caulobacter crescentus*. One copy of the partition complex—a large centromerelike protein cluster bound to the newly replicated chromosome—translocates rapidly from the old to the new cell pole, resulting in chromosome segregation [6]. The translocation of this chromosome-bound cargo depends on a protein gradient: the partition complex follows an increasing amount of ParA in the cell [7–10]. However, the physical principles underlying this directed motion of the partition complex remain unclear.

ParA belongs to the widely conserved ParAB*S* partitioning system for chromosome and plasmid segregation [11]. The ATPase ParA exists in an ADP- and ATP-bound form, and the energy released in ATP hydrolysis is used to generate a nonequilibrium cellular organization of ParA. The preferred location of ParA in the cell depends on its nucleotide state [12]: As an ATP-bound dimer, ParA binds nonspecifically to DNA. On interaction with the ParB partition complex [13–18], its ATPase activity is stimulated, leading to detachment of ADP-bound ParA monomers into the cytosol, thereby producing a ParA gradient around the partition complex. The ATP-dependent interactions of ParA with this cargo are thus necessary for its directed translocation [12], indicating that the ParAB*S* system is an active intracellular transport system.

Various mechanisms have been proposed for force generation [7,19–22], including a class of Brownian-ratchet models [23–27]. Specifically, a DNA-relay mechanism was suggested [23,28], in which DNA-bound ParA proteins relay the partition complex up a ParA concentration gradient by exploiting elastic fluctuations of the chromosome [23,29]. Using simulations, it has been argued that this model can explain the experimentally observed translocation of the partition complex [23,29]. However, a theoretical description of the DNA-relay force that reveals the dependence of the force on key system parameters is still lacking.

In this Letter we present an analytic theory for force generation by the DNA-relay mechanism. We compute the relay force by evaluating the stochastic binding of DNA-bound ParA-like proteins to a cargo using a master equation approach. Conceptually, the predicted relay force originates from the interplay of the ParA gradient, chromosome fluctuations, and an emergent friction force due to the interactions of chromosome-bound ParA proteins with the cargo. These contributions give rise to four distinct force generation regimes, depending on the strength of chromosomal fluctuations and the cytoplasmic friction on the cargo. We thus establish a theoretical framework to characterize the DNA-relay mechanism over a broad range of operational conditions, providing conceptual insight into active directed transport of ParB-like cargos for *in vivo* [23,30–32] and *in vitro* [33] settings.

To elucidate force generation by the DNA-relay mechanism [23,29], we study a minimal model obtained by reducing the full complexity of the partitioning system to

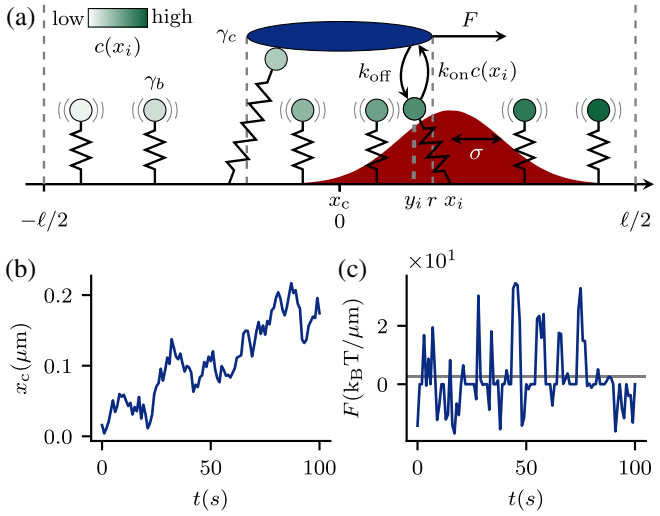

FIG. 1. Minimal model for force generation by DNA relaying. (a) The relay force F arises from the interactions of the cargo with ParA ATPases bound to the chromosome, represented by a set of chromosomal elements modeled as a bead-spring system with an associated ParA concentration (indicated by the green tone). We assume that the ParA gradient is comoving with the cargo. Chromosomal elements fluctuate due to thermal energy, with the magnitude of the fluctuations, $\sigma = \sqrt{k_B T/k}$ (red Gaussian). Our 1D model is presented in 2D for visual purposes. (b),(c) Cargo trajectory (b) and the corresponding DNA-relay force (c) obtained from the numerical solution of Eq. (1) using Brownian dynamics simulation. The horizontal line shows the time average of F.

key elements important for DNA relaying [Fig. 1(a)]. Our one-dimensional model consists of the cargo and ParA-bound chromosomal elements. To account for the chromosomal dynamics in a simplified manner, the chromosome is modeled as a set of fluctuating elastic springs. In ParABS-like partitioning systems, the ATPase ParA detaches from the chromosome at the ParB cargo due to stimulation of ATP hydrolysis by ParB and can rebind to the chromosome only on ATP binding and dimerization. This dynamics results in a ParA gradient propagating with the cargo, as was shown for an *in vitro* reconstituted partitioning system [33,34]. Since our aim is to derive a minimal model for force generation by stochastic ParA-cargo interactions, we use this observation by imposing a comoving ParA gradient on the cargo, instead of modeling the ParA dynamics explicitly.

Specifically, the cargo is represented as a line segment of length $2r$ with a reaction radius r, and chromosomal regions are described in a coarse-grained way as a set of $N_{\rm tot}$ beads, equally spaced along a domain of length ℓ [Fig. 1(a)]. Each bead is tethered to a fixed position by a spring with stiffness k, thermally fluctuating with amplitude $\sigma = \sqrt{k_B T/k}$. The ParA concentration associated with a chromosomal bead at a distance x_i from the cargo is set to $c(x_i) = mx_i + c_0$. Note that the coordinates x_i are defined in the cargo frame of reference, thereby enforcing the comoving ParA gradient. Cargo and chromosomal elements interact: Beads within the reaction radius of the cargo bind with rate $k_{\rm on}c(x)$. Cargo-bound beads unbind with rate $k_{\rm off}$. Importantly, due to the elasticity of the DNA, cargo-bound chromosomal elements exert a force on the cargo. We describe the resulting cargo motion by an overdamped Langevin equation:

$$\gamma_{\rm c}\frac{dx_{\rm c}}{dt} = k\sum_i (x_i - y_i) + \sqrt{2\gamma_{\rm c}k_{\rm B}T}\eta(t), \qquad (1)$$

where $x_{\rm c}$ is the cargo position and the index i runs over all cargo-bound chromosomal elements with rest position x_i and bead position y_i. The white noise term $\eta(t)$ satisfies $\langle\eta(t)\rangle = 0$ and $\langle\eta(t)\eta(t')\rangle = \delta(t-t')$, and $\gamma_{\rm c}$ is the friction coefficient of the cargo in the cytoplasm.

Our goal is to calculate the steady-state DNA-relay force on the cargo for a comoving ParA gradient. To compute the steady-state DNA-relay force using a finite chromosomal domain of size ℓ, we employ periodic boundary conditions, such that there are always $N_{\rm tot}$ chromosomal elements the cargo could interact with (Supplemental Material [35]). For $\sigma \gg \ell$, the limited number of chromosomal elements becomes important, allowing us to study finite system size effects. In contrast, if $\sigma \ll \ell$, this model is effectively identical to one with an infinite system size.

To facilitate further theoretical analysis we recast variables and system parameters in a nondimensional form using the system size ℓ as a characteristic length $x \to x\ell$ and the unbinding time $1/k_{\rm off}$ as characteristic time scale $t \to t/k_{\rm off}$. Using this nondimensionalized form, we identify four key parameters that dictate the system's dynamics: The binding propensity $c_0 k_{\rm on}/k_{\rm off} \to c_0$ characterizes the on/off kinetics between the cargo and ParA; the concentration gradient $m\ell/c_0 \to m$ describes the asymmetry of the ParA gradient on the chromosome; $\sigma/\ell \to \sigma$ sets the magnitude of chromosomal fluctuation relative to system size; and the cargo friction coefficient $\gamma_{\rm c}k_{\rm off}\ell^2/(k_{\rm B}T) \to \gamma_{\rm c}$ provides a measure for how susceptible the cargo is to DNA-relay forces (Supplemental Material [35]).

Using Brownian dynamics simulations [Figs. 1(b) and 1(c)] we find distinct force-generation regimes depending on the magnitude of chromosomal fluctuations σ and the cytoplasmic friction coefficient $\gamma_{\rm c}$ of the cargo, each characterized by a different dependence on σ (Fig. 2). While we observe maximal force under stalling conditions ($\gamma_{\rm c} \to \infty$), the system's behavior changes drastically for a moving cargo (finite $\gamma_{\rm c}$). Interestingly, in this parameter range we find a maximum in the force at intermediate σ, suggesting an optimal operating regime for this transport mechanism.

To provide conceptual insight into the DNA-relay mechanism, we develop an analytical theory to calculate the relay force on the cargo. Specifically, we derive an approximation for the relay force

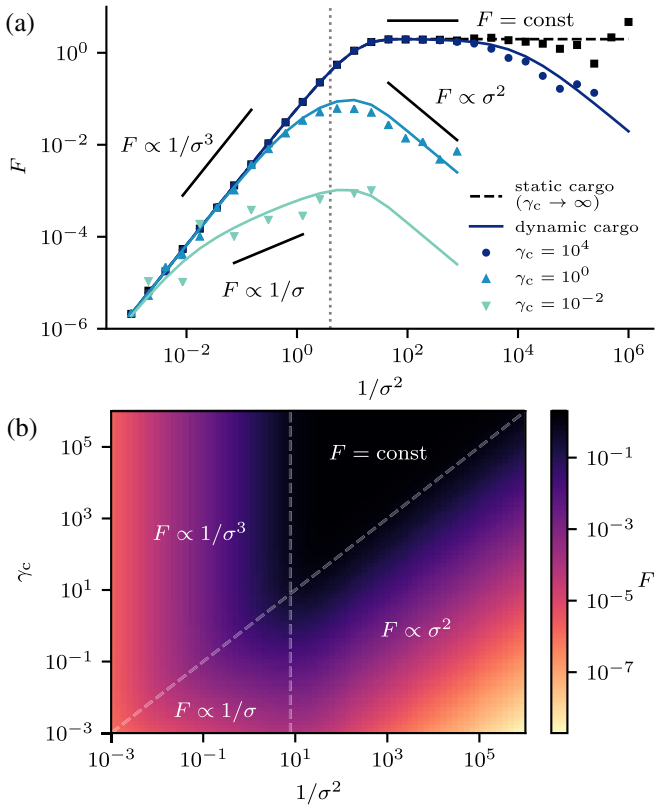

FIG. 2. Average relay force F in the weak-binding limit ($c_0 \ll 1$) for different values of the friction coefficient γ_c of the cargo in the cytoplasm and the magnitude of chromosome fluctuations σ. (a) We compare results from simulations (dots) with theory (lines), obtained from Eqs. (8) and (10) for a static (black) and moving cargo (blue), respectively. The dotted vertical line at $\sigma = 1/2$ separates the different force generation regimes. (b) Phase diagram of force generation regimes.

$$F = \frac{1}{\sigma^2}\sum_i (x_i - y_i), \tag{2}$$

which reveals how microscopic system parameters control the DNA-relay mechanism. To obtain an explicit analytical expression, we consider the average relay force and use a continuum approximation

$$\begin{aligned} F &= \frac{1}{\sigma^2}\int_{-1/2}^{1/2} dx \int_{-r}^{r} dy\, n(x,y,t)(x-y) \\ &= \int_{-1/2}^{1/2} dx\, f(x,t). \end{aligned} \tag{3}$$

We moved to the cargo frame of reference, introduced the density $n(x,y,t)$ of cargo-bound chromosomal elements with a rest position x and binding position y at the cargo, and defined the force density

$$f(x,t) = \frac{1}{\sigma^2}\int_{-r}^{r} dy\, n(x,y,t)(x-y). \tag{4}$$

Thus, the relay force can be understood by studying the force density f, for which we need to calculate $n(x,y,t)$.

The dynamics of the density $n(x,y,t)$ is described by

$$\begin{aligned} &\partial_t n(x,y,t) - v(n,t)\partial_x n(x,y,t) \\ &\quad = c(x)\phi(y;x,\sigma)[N_{\text{tot}} - n(x,t)] - n(x,y,t). \end{aligned} \tag{5}$$

For a static cargo ($v = 0$), the temporal change in n is determined only by a gain and a loss term, corresponding to binding to and unbinding from the cargo. For a binding event, a chromosomal bead needs to move within the reaction radius of the cargo. We describe the position y of an unbound bead as a Gaussian random variable with mean x and variance σ^2. The probability that a bead with rest position x is at position $y \in [-r, r]$ is thus given by the Gaussian probability density function $\phi(y;x,\sigma)$ [Fig. 1(a)]. This is justified under weak chromosome-cargo interactions, i.e., whenever the decorrelation time $\tau_{\text{corr}} = \sigma^2\gamma_b N_{\text{tot}}$ is much smaller than the binding time $\tau_{\text{bind}} = 1/c_0$. A binding event takes place stochastically with a rate $c(x)[N_{\text{tot}} - n(x,t)]$, accounting for the finite density of chromosomal elements available for binding, where $c(x) = c_0(1 + mx)$ denotes the dimensionless ParA concentration. The total density of cargo-bound chromosomal beads with rest position x can be obtained by integrating the density $n(x,y,t)$ over all possible binding positions y on the cargo:

$$n(x,t) = \int_{-r}^{r} dy\, n(x,y,t). \tag{6}$$

Unbinding is described by a constant detachment rate, set by the last term in Eq. (5). Finally, when $v \neq 0$ the temporal evolution of n also includes an advection term to account for cargo motion.

We expect the weak-binding limit ($c_0 \ll 1$) to be the biologically relevant parameter regime in this model, because of the high ParA turnover rate caused by ParB-induced ATP hydrolysis of ParA and subsequent detachment of ParA from the cargo [36]. Henceforth, we thus consider only this limit, for which saturation effects of the cargo by bound chromosomal elements are negligible. For completeness, we provide our results for the strong-binding limit (Supplemental Material [35]) and find that the conceptual insights gained from the weak-binding limit largely apply.

Having established a theoretical framework to study force generation by DNA relaying, we first consider the case of a static cargo ($v = 0$). Put simply, we compute the stalling force of the cargo. This static case allows us to study basic features of the force generation mechanism and provides insights that will also be relevant for the moving cargo scenario. We first calculate the steady-state solution of Eq. (5), and with this an expression for the steady-state force density (Supplemental Material [35]):

$$f(x) = N_{\mathrm{tot}} c(x)[\phi(x; r, \sigma) - \phi(x; -r, \sigma)]. \quad (7)$$

This expression for the force density constitutes one of our key findings and allows us to understand how the DNA-relay force is generated and how it depends on system parameters.

The force density encodes the contribution of a chromosomal element with rest position x to force generation. Intuitively, this force density is determined by the interplay between how likely it is for a chromosomal element to bind to the cargo and how much force is exerted on the cargo in this configuration. In the limit $\sigma \gg 1$, chromosomal beads exhibit strong fluctuations, and without a ParA gradient ($m = 0$) every bead thus has approximately the same binding probability. Here, only the distance of a chromosomal element from the cargo matters for force generation and therefore the force density increases linearly with the distance of the bead from the cargo [Fig. 3(a), light green]. Because of the symmetry of $f(x)$, forces exerted on the cargo from chromosomal elements positioned behind and in front of the cargo cancel, such that no net force is generated. By contrast, if the ParA concentration on the beads increases toward the right ($m > 0$), beads in front of the cargo are more likely to bind to the cargo than those behind. Hence, the force density profile starts to deviate from an odd function, resulting in a net positive force [Fig. 3(a), dark green). In the regime $\sigma \ll 1$ there is a nonuniform probability for chromosomal beads to bind to the cargo. While chromosomal elements far from the cargo are less likely to bind, they generate the largest force contribution. Consequently, the force density peaks at an intermediate position between the cargo edge and the system boundary [Fig. 3(b)]. These maximal force density values are, for the parameters shown in Fig. 3, three orders of magnitude larger than those observed for $\sigma \gg 1$. Again, in the presence of a ParA gradient $f(x)$ deviates from being an odd function, resulting in a net force on the cargo. In all cases, our analytical predictions for the force density are in accord with Brownian dynamics simulations.

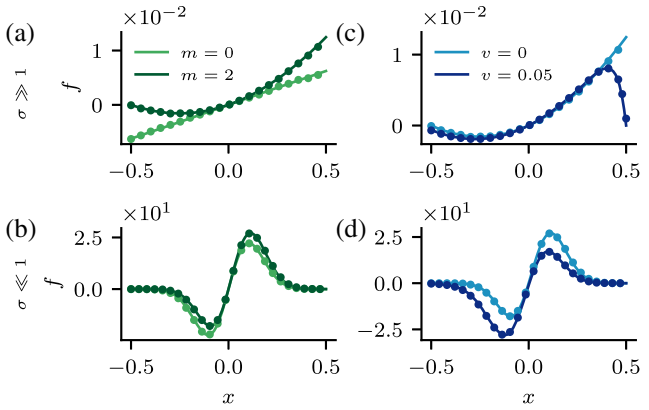

FIG. 3. The influence of the ParA concentration gradient m and the cargo velocity v on the force density $f(x)$. (a),(b) $f(x)$ for a static cargo given by Eq. (7) without ($m = 0$) and with ($m = 2$) a ParA gradient. (c),(d) $f(x)$ for a static ($v = 0$) and a moving ($v = 0.05$) cargo both with $m = 2$. The force density for a moving cargo is obtained numerically. We compare results from simulations (dots) and our theoretical results (lines). Note that the dark green and the light blue curves in (a),(c) and (b),(d) show the same data.

Having analyzed the steady-state force density $f(x)$, we next evaluate the cargo stalling force F_{sc} in the weak-binding limit using Eq. (3):

$$F_{\mathrm{sc}} = \int_{-1/2}^{1/2} dx\, N_{\mathrm{tot}} c(x)[\phi(x; r, \sigma) - \phi(x; -r, \sigma)]. \quad (8)$$

On performing this integral, we obtain the dependence of the cargo stalling force on σ (Fig. 2). Remarkably, for $\sigma \ll 1$ we find that F_{sc} is independent of σ. On increasing σ, more chromosomal elements are recruited to contribute to force generation. However, this increase in participation is precisely compensated by the softening of the springs resulting in a stiffness independent DNA-relay force $F_{\mathrm{sc}} = \mathrm{const}$. For $\sigma \gg 1$, we obtain $F_{\mathrm{sc}} \propto 1/\sigma^3$. Here, the finite size of the system affects force generation. Because of the limited number of beads, the softening of the springs can not be compensated anymore by an increased amount of beads interacting with the cargo. Therefore, the force on the cargo decreases.

To understand force generation for a dynamic cargo, we first consider the case of a cargo that moves with an imposed velocity v. To this end, we study the steady-state force density, which determines the relay force $F(v)$. We calculate the steady-state solution of Eq. (5) for a fixed velocity v and obtain the corresponding force density $f(x)$ using Eq. (4). We observe that, for $v > 0$, the weight of the binding profile is relocated from the leading (right) to the lagging (left) side of the cargo [Figs. 3(c) and 3(d), dark blue). This can be understood intuitively: In the case of a dynamic cargo, the forward movement of the cargo and the finite time a chromosomal bead is attached to the cargo (on average $1/k_{\mathrm{off}}$) result in an increased amount of chromosomal beads pulling the cargo backward.

Interestingly, we find that a moving cargo experiences the force

$$F(v) = F_{\mathrm{sc}} - v\frac{1}{\sigma^2} N_{\mathrm{sc}}, \quad (9)$$

which has two contributions: the static relay force and an additional force term linear in v. This term can be interpreted as an emergent friction force with the friction coefficient $\gamma_{\mathrm{e}} = (1/\sigma^2) N_{\mathrm{sc}} = (1/\sigma^2) 2rc_0$, where N_{sc} denotes average number of cargo bound beads for a static cargo (Supplemental Material [35]).

Next, we use this result for imposed motion to obtain the DNA-relay force exerted on a cargo that moves autonomously due to diffusion and the interactions with ParA-bound beads. First, we self-consistently determine the velocity v of a self-propelled cargo using force balance $\gamma_c v = F(v)$. From this analysis, we obtain an explicit expression for the generated force associated to this translocation velocity:

$$F = \frac{F_{sc}}{1 + \frac{\gamma_e}{\gamma_c}}. \tag{10}$$

Interestingly, the force on an autonomously moving cargo can be entirely calculated from quantities obtained for a static cargo.

The interplay of self-propulsion and emergent friction force gives rise to four distinct force generation regimes, as depicted in the phase diagram in Fig. 2(b). As in the static limit, we distinguish force generation for small and large chromosomal fluctuations. Importantly, however, the qualitative dependencies on the strength of the chromosome fluctuations can differ because of the emergent friction force. When the cytoplasmic friction dominates the emergent friction, $\gamma_c \gg \gamma_e$, the dynamic relay force is well approximated by the static relay force [Fig. 2(a), black line]. On lowering the cytoplasmic friction slightly, the emergent friction reduces force generation only for small σ. Here, the σ dependence of the emergent friction, $\gamma_e \propto 1/\sigma^2$, combines with the constant static cargo force to $F \propto \sigma^2$ [Fig. 2(a), dark blue line]. On lowering γ_c further, the emergent friction also influences the regime $\sigma \gg 1$. For this parameter regime, the decrease in driving and friction force with increasing σ combine to $F \propto 1/\sigma$ [Fig. 2(a), light blue line]. In the limit $\sigma \to \infty$, we find that the relay force vanishes, as for a static cargo. Importantly, we find that these force generation regimes emerge robustly also in the case of more general nonlinear concentration profiles (Supplemental Material [35]). In all cases, we find that our analytical predictions agree well with Brownian dynamics simulations.

Our work complements previous studies on numerically and phenomenologically modeling cargo motion in ParAB*S*-like systems [23–26,29,37,38] by providing an analytical microscopic theory for force generation by DNA relaying. It is still debated whether the main contribution to force generation in ParAB*S* systems derives from chromosome elasticity (DNA-relay force) [23–26,28] or chemophoresis [22,27,39]. We contribute to this open question by developing a quantitative mechanistic theory. Our analytical predictions for the dependence of the DNA-relay force on microscopic parameters could be tested in *in vitro* experiments with a stiffness controlled DNA carpet [33]. We find that the relay force depends on the friction coefficient of the cargo in the cytoplasm, which varies with the size of the cargo and cytoplasm composition. Hence, this observation could be explored *in vitro* by considering differently sized cargoes or adding crowding agents to the system. Furthermore, our relation for the emergent friction coefficient could be tested experimentally by varying the amount of ParA in the system. An increased concentration of ParA should result in more cargo-bound ParA and hence a larger emergent friction coefficient. In future work, our framework can serve as a starting point for further investigations of force generation in ParAB*S* systems with complex ParA dynamical patterns [19] and nonequilibrium activity in the chromosome [40,41]. Our theory might also be useful more generally for macroscopic cargo translocation driven by stochastic interactions, as observed both in prokaryotic and eukaryotic cells [42–44].

This research was funded by the Deutsche Forschungsgemeinschaft (DFG, German Research Foundation) via Project No. 269423233 - TRR 174 and via a fellowship through the Graduate School of Quantitative Biosciences Munich (S. B. and E. F.). C. H. acknowledges support by the Studienstiftung des deutschen Volkes (German Academic Scholarship Foundation) and thanks the Max Planck Institute for the Physics of Complex Systems, Dresden (Germany) for hospitality.

*These authors contributed equally to this work.
†c.p.broedersz@vu.nl

[1] I. V. Surovtsev and C. Jacobs-Wagner, Cell **172**, 1271 (2018).
[2] E. Toro and L. Shapiro, Cold Spring Harbor Perspect. Biol. **2**, a000349 (2010).
[3] D. Schumacher, S. Bergeler, A. Harms, J. Vonck, S. Huneke-Vogt, E. Frey, and L. Søgaard-Andersen, Dev. Cell **41**, 299 (2017).
[4] M. A. J. Roberts, G. H. Wadhams, K. A. Hadfield, S. Tickner, and J. P. Armitage, Proc. Natl. Acad. Sci. U.S.A. **109**, 6698 (2012).
[5] D. F. Savage, B. Afonso, A. H. Chen, and P. A. Silver, Science **327**, 1258 (2010).
[6] R. B. Jensen and L. Shapiro, Proc. Natl. Acad. Sci. U.S.A. **96**, 10661 (1999).
[7] J. L. Ptacin, S. F. Lee, E. C. Garner, E. Toro, M. Eckart, L. R. Comolli, W. Moerner, and L. Shapiro, Nat. Cell Biol. **12**, 791 (2010).
[8] W. B. Schofield, H. C. Lim, and C. Jacobs-Wagner, EMBO J. **29**, 3068 (2010).
[9] C. W. Shebelut, J. M. Guberman, S. van Teeffelen, A. A. Yakhnina, and Z. Gitai, Proc. Natl. Acad. Sci. U.S.A. **107**, 14194 (2010).
[10] I. V. Surovtsev, H. C. Lim, and C. Jacobs-Wagner, Biophys. J. **110**, 2790 (2016).
[11] J. Livny, Y. Yamaichi, and M. K. Waldor, J. Bacteriol. **189**, 8693 (2007).
[12] J. Lutkenhaus, Trends Microbiol. **20**, 411 (2012).
[13] C. P. Broedersz, X. Wang, Y. Meir, J. J. Loparo, D. Z. Rudner, and N. S. Wingreen, Proc. Natl. Acad. Sci. U.S.A. **111**, 8809 (2014).

[14] D. A. Mohl and J. W. Gober, Cell **88**, 675 (1997).
[15] H. Murray, H. Ferreira, and J. Errington, Mol. Microbiol. **61**, 1352 (2006).
[16] A. M. Breier and A. D. Grossman, Mol. Microbiol. **64**, 703 (2007).
[17] R. E. Debaugny, A. Sanchez, J. Rech, D. Labourdette, J. Dorignac, F. Geniet, J. Palmeri, A. Parmeggiani, F. Boudsocq, V. Anton Leberre, J. Walter, and J. Bouet, Mol. Syst. Biol. **14**, e8516 (2018).
[18] A. Sanchez, D. Cattoni, J.-C. Walter, J. Rech, A. Parmeggiani, M. Nollmann, and J.-Y. Bouet, Cell Syst. **1**, 163 (2015).
[19] S. Ringgaard, J. van Zon, M. Howard, and K. Gerdes, Proc. Natl. Acad. Sci. U.S.A. **106**, 19369 (2009).
[20] E. J. Banigan, M. A. Gelbart, Z. Gitai, N. S. Wingreen, and A. J. Liu, PLoS Comput. Biol. **7**, e1002145 (2011).
[21] B. Shtylla and J. P. Keener, J. Theor. Biol. **307**, 82 (2012).
[22] T. Sugawara and K. Kaneko, Biophysics **7**, 77 (2011).
[23] H. C. Lim, I. V. Surovtsev, B. G. Beltran, F. Huang, J. Bewersdorf, and C. Jacobs-Wagner, eLife **3**, e02758 (2014).
[24] L. Hu, A. G. Vecchiarelli, K. Mizuuchi, K. C. Neuman, and J. Liu, Proc. Natl. Acad. Sci. U.S.A. **112**, E7055 (2015).
[25] L. Hu, A. G. Vecchiarelli, K. Mizuuchi, K. C. Neuman, and J. Liu, Biophys. J. **112**, 1489 (2017).
[26] L. Hu, A. G. Vecchiarelli, K. Mizuuchi, K. C. Neuman, and J. Liu, Plasmid **92**, 12 (2017).
[27] J.-C. Walter, J. Dorignac, V. Lorman, J. Rech, J.-Y. Bouet, M. Nollmann, J. Palmeri, A. Parmeggiani, and F. Geniet, Phys. Rev. Lett. **119**, 028101 (2017).
[28] P. A. Wiggins, K. C. Cheveralls, J. S. Martin, R. Lintner, and J. Kondev, Proc. Natl. Acad. Sci. U.S.A. **107**, 4991 (2010).
[29] I. V. Surovtsev, M. Campos, and C. Jacobs-Wagner, Proc. Natl. Acad. Sci. U.S.A. **113**, E7268 (2016).
[30] R. Ietswaart, F. Szardenings, K. Gerdes, and M. Howard, PLoS Comput. Biol. **10**, e1004009 (2014).
[31] D. Schumacher and L. Søgaard-Andersen, Annu. Rev. Microbiol. **71**, 61 (2017).
[32] A. Le Gall, D. I. Cattoni, B. Guilhas, C. Mathieu-Demazière, L. Oudjedi, J.-B. Fiche, J. Rech, S. Abrahamsson, H. Murray, J.-Y. Bouet, and M. Nollmann, Nat. Commun. **7**, 12107 (2016).
[33] A. G. Vecchiarelli, K. C. Neuman, and K. Mizuuchi, Proc. Natl. Acad. Sci. U.S.A. **111**, 4880 (2014).
[34] L. C. Hwang, A. G. Vecchiarelli, Y.-W. Han, M. Mizuuchi, Y. Harada, B. E. Funnell, and K. Mizuuchi, EMBO J. **32**, 1238 (2013).
[35] See Supplemental Material at http://link.aps.org/supplemental/10.1103/PhysRevLett.127.138101 for a detailed derivation.
[36] A. G. Vecchiarelli, Y.-W. Han, X. Tan, M. Mizuuchi, R. Ghirlando, C. Biertümpfel, B. E. Funnell, and K. Mizuuchi, Mol. Microbiol. **78**, 78 (2010).
[37] L. Jindal and E. Emberly, PLoS One **14**, e0218520 (2019).
[38] S. Bergeler and E. Frey, PLoS Comput. Biol. **14**, e1006358 (2018).
[39] L. Jindal and E. Emberly, PLoS Comput. Biol. **11**, e1004651 (2015).
[40] F. S. Gnesotto, F. Mura, J. Gladrow, and C. P. Broedersz, Rep. Prog. Phys. **81**, 066601 (2018).
[41] S. C. Weber, A. J. Spakowitz, and J. A. Theriot, Proc. Natl. Acad. Sci. U.S.A. **109**, 7338 (2012).
[42] B. Sabass and U. S. Schwarz, J. Phys. Condens. Matter **22**, 194112 (2010).
[43] M. Srinivasan and S. Walcott, Phys. Rev. E **80**, 046124 (2009).
[44] N. Saito and K. Kaneko, Sci. Rep. **7**, 44288 (2017).